Identification of fracture properties at the interface between CMC and EBC at room and high temperatures using full field measurements

Pierre Bertrand, Cédric Huchette, Thibaut Archer, Thomas Vandellos, François Hild

IDENTIFICATION OF FRACTURE PROPERTIES AT THE INTERFACE BETWEEN CMC AND EBC AT ROOM AND HIGH TEMPERATURES USING FULL FIELD MEASUREMENTS

Pierre Bertrand[123], Cédric Huchette[2], Thibaut Archer[2], Thomas Vandellos[1] and François Hild[3]

[1]Safran Ceramics, a technology platform of Safran Tech, Le Haillan, France
pierre.bertrand@onera.fr
thomas.vandellos@safrangroup.com
[2]DMAS, ONERA, Université Paris-Saclay, Chatillon, France
cedric.huchette@onera.fr
thibaut.archer@onera.fr
[3]Université Paris-Saclay, CentraleSupélec, ENS Paris-Saclay, CNRS
LMPS–Laboratoire de Mécanique Paris-Saclay, Gif sur Yvette, France
francois.hild@ens-paris-saclay.fr

Keywords: Ceramic Matrix Composite, Environmental Barrier Coating, Digital Image Correlation, test/finite element simulation dialogue, interfacial crack propagation

Abstract
The objective of this work is to predict the lifespan of CMC/EBC systems by quantifying interface damage and estimating the interface adhesion energy. Four-point flexural tests were conducted at room temperature and 1000°C. These tests initiated cracks through the thickness of the coating. Then, the crack bifurcated and propagated along the interface. Visible light cameras (monovision and stereovision) monitored these tests to measure kinematic fields via digital image correlation (DIC). The kinematic fields were used to establish a test/finite element (FE) simulation dialogue to estimate the crack tip locations at the substrate/coating interface. Experimental displacement fields are also used as input in FE simulations (applying boundary conditions from DIC-derived fields) to calculate the critical energy release rate at the interface during crack propagation. Initially implemented for room temperature test, these methods are then applied to a high-temperature test. The computed energy release rates for both temperatures indicate higher interfacial fracture toughness at elevated temperatures.

1. Introduction

Ceramic Matrix Composites (CMCs) are increasingly employed in the aerospace industry, notably by engine manufacturers. SiC/SiC CMCs are currently studied as an alternative to metallic alloys in hot sections of engines thanks to their low density and excellent mechanical properties at high temperatures. CMCs enable engine performances to be improved to reduce fuel consumption. In engine environments, the CMC components face severe physicochemical conditions (*e.g.* oxidation, corrosion) that may induce critical damage mechanisms such as SiC recession impacting the lifespan. To protect CMC components, Environmental Barrier Coatings (EBCs) have been developed to achieve various functions (*e.g.* protection against corrosion, thermal barrier, CMAS resistance). The considered coating comprises multiple layers, namely, a Silicon bonding layer and an Yttrium Disilicate protective layer. This coating may experience different damage mechanisms in engine environments, with interface delamination being the most critical one, rendering CMCs vulnerable to SiC recession. Thus, preventing and understanding delamination is crucial for designing these coated composites.

To characterize the delamination of interfaces and their adhesion, it is interesting to rely on the quantification of fracture toughness, which is based on the stress state close to the crack tip with stress intensity factors K [1] or based on the energy needed to create a new surface with the energy realease rate G [2]. Here the choice was made to evaluate the fracture toughness with the critical energy release rate G_C. In order to compute this quantity of interest, one may design a test where a crack located at the interface is propagating in a stable manner. To achieve such propagation many experimental setups were proposed in the literature including tension [3, 4], compression [5, 6], shear loading [7, 8], indentation [9] and flexural [10 ,11, 12, 13, 14, 15] tests. Among these tests, four-point flexure appears adapted to characterize the adhesion of stiff bimaterials. It was used, for instance, to quantify the adhesion between an aluminum alloy and a polymer layer [10], metallic alloys and ceramic thermal barrier coating (TBC) [11], [13] but also on CMC/EBC systems [14]. Because of the small thickness of the coating, an additional plate stiffening layer on the coated surface is needed to bring additional elastic energy to the system to drive interfacial crack propagation. This additional plate prevents from performing the test at high temperature. To overcome this challenge, three-points flexural tests were performed at 800°C on a metallic alloy with a thermal barrier ceramic coating without the need for a stiffener [16]. To ensure that the crack is located at the interface, the thickness of the coating layer is increased to move the interface in the direction of the neutral axis With this geometry, when the mechanical load is applied, a transverse crack is initiated in the coating that is submitted to tensile stresses. Once the transverse crack reaches the interface, it bifurcates and propagates along the interface. It is reported that interfacial cracks propagate slowly and steadily. To follow the cracks propagation and identify the position of the crack tip to compute the critical energy release rate G_C, the flexural test was intrumented with a camera positioned outside of the furnace as illustrated in **Figure 1**. The acquired images were used to perform Digital Image Correlation (DIC) to measure kinematic fields. The strain field is then used to assess the crack length to compute G_C with the compliance method.

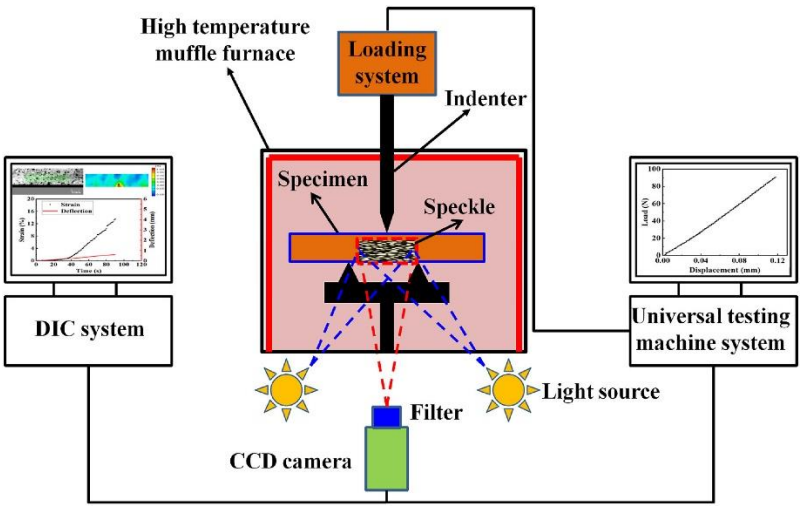

Figure 1. Three-point flexural test setup at high temperature with a camera to perform DIC [16].

In the following, four-point flexural tests were performed on a CMC/EBC system to initiate and propagate stable cracks at the interface. The coating thickness was of the same order of magnitude as the one of the substrate. It was decided to perform four-point flexural tests instead of three-point flexural tests because studies showed that delamination was more likely to be stable, for instance, in End-Notched Flexure (ENF) [17] and higher shear stresses at the interface in a four-point configuration make it easier for cracks to bifurcate and propagate. The four-point flexural tests were performed at room temperature and at 1000°C in a furnace. In both cases, the tests were instrumented with cameras. Experimental displacement field were measured via DIC and used to drive Finite Element (FE) simulations. This procedure allows for the identification of the crack length at the interface as well as for the computation of the critical energy release rate. The fracture toughness obtained at room temperature is compared to its level at high temperature.

2. Materials and method

2.1. Experimental setup

The four-point flexural tests were performed on a parallelepipedic sample illustrated in **Figure 2**. With a width of 10 mm, a 2.7 mm thick CMC substrate on top of which a 2.0 mm thick EBC made of rare earth disilicate was deposited by thermal projection. The CMC/EBC plates were cut at the desired length (*i.e.* the samples were about 10 mm longer than the distance between the outer flexural supports).

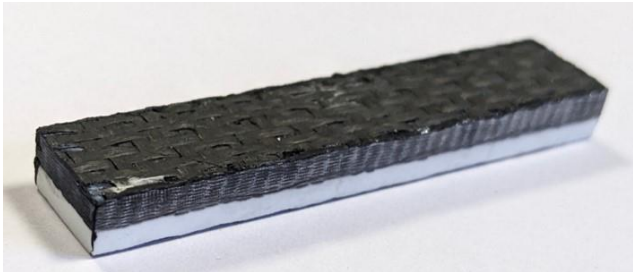

Figure 2. CMC/EBC flexural sample.

The flexural setups used at both temperatures are presented in **Figure 3**. The geometries were slightly different, the distances between the inner/outter rollers were 25 mm / 60 mm at room temperature, and 16 mm / 32 mm at high temperature. The four-point flexural tests were performed on a servohydraulic Instron testing machine with a constant crosshead speed of 0.25 mm / min at room temperature and 0.1 mm / min at high temperature.

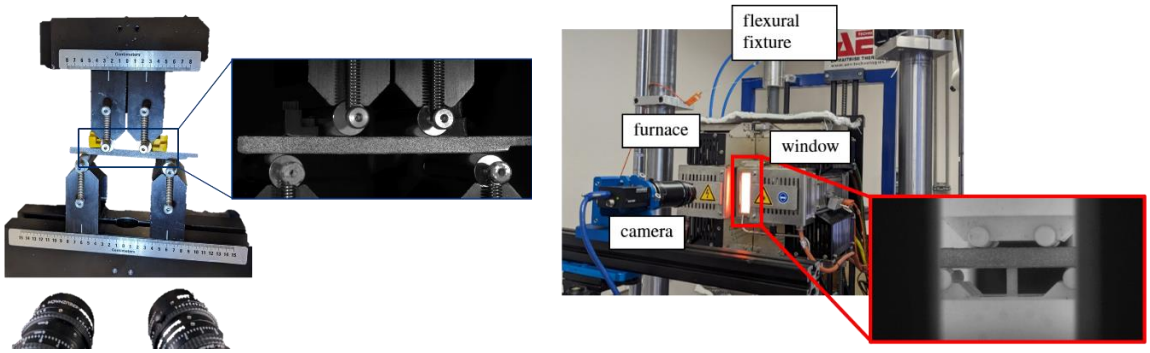

(a) **(b)**

Figure 3. Four-point flexural setups with the associated instrumentation (a) at room and (b) at high temperatures.

During the tests, four different stages were observed. During the first stage, after a nonlinear response due to the contact of the rollers on the sample surface, a linear elastic response occurred. During the second phase, a force drop appeared. This nonlinearity corresponds to the initiation of a crack on the surface of the EBC and its propagation along the thickness of the coating. This propagation was unstable. Once the interface was reached, the crack bifurcated and two cracks propagated along the interface. During the third stage, the two cracks propagated steadily until the final fracture of the CMC substrate (fourth stage). These four stages are illustrated on the force/image number curve in **Figure 4**. A similar behavior is observed at room temperature and at high temperature. There was only one transverse crack that initiated during the test at room temperature and two transverse cracks at high temperature. As the geometry of the flexural device was not the same in the two configurations, the force at which the

transverse cracks initiated were not the same. The most interesting stage is the third one because the interfacial fracture toughness could be characterized during the stable propagation of the interfacial crack.

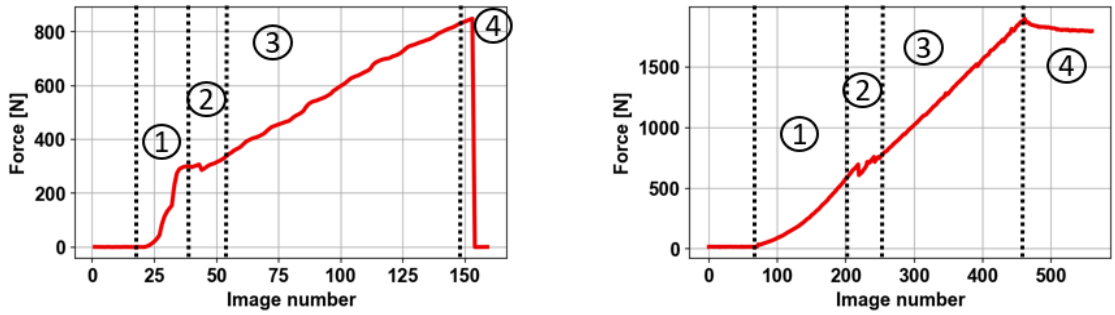

(a) **(b)**

Figure 4. Experimental force as a function of image number acquired during the tests (a) at room and (b) high temperatures.

2.2. Full field measurement via DIC

In the present analyses, FE-based DIC was used to measure kinematic fields [18]. Such formulation of the displacement field is very convenient to transfer fields from experiment to simulation and to compare them. The presence of a crack inside the specimen is characterized by high gradients in the displacement field and high gray level residuals as illustrated in **Figure 5** for the test performed at room temperature.

(a) **(b)**

Figure 5. Transverse and interfacial cracks revealed with (a) the vertical displacement field (expressed in mm) and (b) the gray level residual field.

At high temperature, a new challenge arose, namely, the perturbation of the measured displacement fields due to heat haze effects. This optical phenomenon is caused by variations in the refractive index of air in the observed environment especially in furnaces [19]. Those spurious motions will have an impact in the following analyses.

3. Results

3.1 Crack length identification and validation

The crack length was identified by a dialogue loop between experiment and simulations [20]. The goal is to minimize the gap between experimental and computed displacement fields when a crack is inserted in the mesh by node splitting. The gap is evaluated for various crack lengths and when a minimum is reached the corresponding crack length is considered to be the one that reproduces at best the kinematics. The interest of this method is to perform the minimization on a local model built around each crack, which allows for different numbers of interfacial cracks depending on the considered test. The identified crack lengths are shown in **Figure 6** for both temperatures.

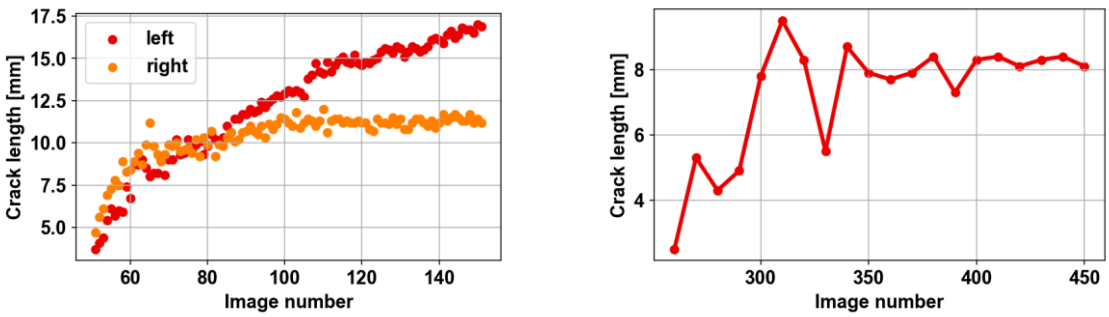

(a) **(b)**

Figure 6. Crack length histories at (a) room and (b) high temperatures.

For the test at 1000°C, only one interfacial crack was considered as the other one did not propagate after bifurcation. **Figure 6(b)** illustrates the impact of heat haze effects on the crack length identification. As the load was constantly increased during the test, the crack should grow with the image number.
To validate the identified crack lengths, the experimental global responses are compared with those obtained with the FE simulations (**Figure 7**). The experimental forces are compared with the vertical reaction forces on the nodes corresponding to the lower contact points where experimentally measured displacements were applied as boundary conditions.

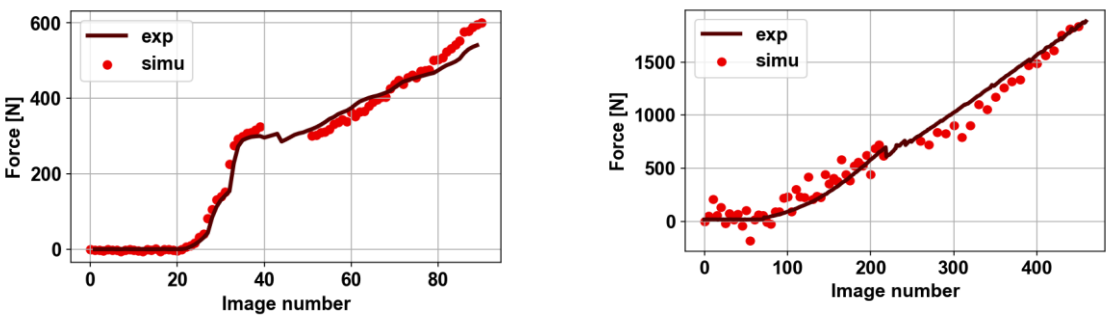

(a) **(b)**

Figure 7. Experiment (exp) /simulation (simu) comparison of the global response of the system at (a) room and (b) high temperatures.

A good correlation is observed between experiments and simulation at room temperature, the loss of global stiffness was well reproduced when the cracks were inserted in the mesh. These results validate the identified crack lengths. At high temperature, the global behavior is well reproduced but some fluctuations are observed, which were mainly due to heat haze effects.

3.2 Energy release rate

The crack length identification and its validation allowed for the evaluation of the critical energy release rate at the interface. This quantity of interest was computed numerically with the J-integral [21] as implemented in Abaqus Standard. The mesh was refined in the vicinity of the crack tip to capture stress intensification in that zone. The values of G_C computed at room and high temperatures are reported in **Table 1**.

Table 1. Energy release rates for both temperatures.

	Room temperature	High temperature
Maximum value of G_C $(J.m^{-2})$	67	209
Standard deviation of G_C $(J.m^{-2})$	16	115

The critical energy release rate is higher at 1000°C than at room temperature by a factor of 3 during crack propagation. This result was also abserved on metallic alloys coated with a thermal barrier [16]. This phenomenom may be explained by nonlinearities close to the crack tip amplified by high temperature conditions or other dissipative phenomena such as creep.

5. Conclusion and perspectives

Four-point flexural tests were performed on CMC/EBC systems at room temperature and at 1000°C in a furnace. This test configuration proved its reliability to initiate and propagate stable cracks at the interface between the CMC and the EBC to evaluate the interfacial fracture toughness. Both tests were analyzed thanks to DIC, which allowed for the crack length identification and energy release rate computation with a close dialogue between experiments and simulations. The comparison of the global response between experiments and simulations was more challenging for the test performed at high temperature because of perturbations in the displacement field measurement due to heat haze effects. The evaluation of the energy release rate during stable crack propagation, which is directly linked to a measure of the energy of adhesion of the interface, showed that the interface was on average tougher at high temperature than at room temperature.

To mitigate the perturbations induced by heat haze effects on the displacement fields, various approaches may be considered. Experimentally, some studies showed that air flow may be a solution to homogenize the temperature and thus the refractive index of the environment [22]. Such device is challenging to integrate in a furnace where insulation from the exterior is key to maintaining high temperatures close to the sample. Other solutions are considered as future work in this study such as using spatiotemporal regularization in DIC analyses [23]. This approach has proven its efficiency to filter-out heat haze contributions by considering global temporal interpolations over a whole time domain instead of performing instantaneous DIC where two pictures are correlated for each time step. Another solution is to rely on integrated DIC where the kinematic basis is tuned to the performed test and the number of degrees of freedom is reduced. This new form of spatial regularization showed its benefits to reduce heat haze effects and to lower uncertainty levels on full field measurement at very high temperatures [24].

Acknowledgments
This work was supported under the ATLAAS framework, a French research project cofounded by DGAC, ONERA and SAFRAN Group, involving SAFRAN Group, ONERA and CNRS.

References

[1] G. R. Irwin. Analysis of Stresses and Strains Near the End of a Crack Traversing a Plate . *Journal of Applied Mechanics*, vol. 24, nº 3, p. 361-364, 2021.
[2] A. Griffith. *The Phenomena of Rupture and Flow in Solids*. Royal Society of London, 1921.
[3] M. P. K. Turunen, P. Marjamäki, M. Paajanen, J. Lahtinen and J. K. Kivilahti. Pull-off test in the assessment of adhesion at printed wiring board metellisation/epoxy interface. *Microelectronics Reliability*, vol. 44, nº 6, p. 993-1007, 2004.
[4] T. Vandellos, M. Hautier, N. Carrere and C. Huchette. Development of a new fracture test to identify the critical energy release rate: The Tensile Flexure test on Notched Specimen. *Engineering Fracture Mechanics*, vol. 96, p. 641-655, 2012.
[5] W. Zhu, L. Yang, J. W. Guo, Y. C. Zhou and C. Lu. Determination of interfacial adhesion energies of thermal barrier coatings by compression test combined with a cohesive zone finite element model. *International Journal of Plasticity*, vol. 64, p. 76-87, 2015.
[6] S. V. Nair, H. E. Eaton and E. Y. Sun. Measurements of interface strength and toughness in shear of environmental barrier coatings on ceramic substrates at ambient and at elevated temperature. *Surface and Coatings Technology*, vol. 200, nº 18, p. 5175-5180, 2006.
[7] Y. Aoki, J. Inoue, Y. Kagawa and K. Igashira. A simple method for measurement of shear delamination toughness in environmental barrier coatings. *Surface and Coatings Technology*, vol. 321, p. 213-218, 2017.
[8] E. Kawai, H. Kakisawa, A. Kubo, N.Yamagushi, T. Yokoi, T.Akatsu, S.Kitaoka and Y.Umeno. Crack Initiation Criteria in EBC under Thermal Stress. *Coatings*, vol. 9, nº 11, Art. nº 11, p. 697, 2019.
[9] J. Yan, T. Leist, M. Bartsch, and A. M. Karlsson. On cracks and delaminations of thermal barrier coatings due to indentation testing: Experimental investigations. *Acta Materialia*, vol. 56, nº 15, p. 4080-4090, 2008.
[10] P. G. Charalambides, J. Lund, A. G. Evans and R. M. McMeeking.A Test Specimen for Determining the Fracture Resistance of Bimaterial Interfaces. *Journal of Applied Mechanics*, vol. 56, nº 1, p. 77-82, 1989.
[11] I. Hofinger, M. Oechsner, H.-A. Bahr and M. V. Swain. Modified four-point bending specimen for determining the interface fracture energy for thin, brittle layers. *International Journal of Fracture*, vol.92, p. 8, 1998.
[12] Y. Zhao, A. Shinmi, X. Zhao, P.J. Withers, S. Van Boxel, N. Markocsan, P. Nylen and P. Xiao. Investigation of interfacial properties of atmospheric plasma sprayed thermal barrier coatings with four-point bending and computed tomography technique. *Surface and Coatings Technology*, vol. 206, nº 23, p. 4922-4929, 2012.
[13] J.-R. Vaunois, M. Poulain, P. Kanouté and J.-L. Chaboche. Development of bending tests for near shear mode interfacial toughness measurement of EB-PVD thermal barrier coatings. *Engineering Fracture Mechanics*, vol. 171, p. 110-134, 2017.
[14] B. T. Richards, D. Zhu, L. J. Ghosn and H. N. G. Wadley. Mechanical Properties of Air Plasma Sprayed Environmental Barrier Coating (EBC) Systems: Preliminary Assessments. *Developments in Strategic Ceramic Materials*, John Wiley & Sons, Ltd, p. 219-237, 2015.
[15] M. Fernandez, G. Couégnat and F. Rebilla. Relation entre oxydation et évolution de l'adhérence d'une barrière environnementale. In *Journées Nationales sur les Composites*, 2019.
[16] W. Zhu, Q. Wu, L. Yang and Y. C. Zhou. In situ characterization of high temperature elastic modulus and fracture toughness in air plasma sprayed thermal barrier coatings under bending by using digital image correlation. *Ceramics International*, vol. 46, nº 11, Part B, p. 18526-18533, 2020.

[17] T. Vandellos. Développement d'une stratégie de modélisation du délaminage dans les structures composites stratifiées. PhD from University Bordeaux 1, 2011.
[18] F. Hild and S. Roux. Comparison of Local and Global Approaches to Digital Image Correlation. *Exp Mech*, vol. 52, nº 9, p. 1503-1519, 2012.
[19] A. Delmas, Y. le maoult, J.-M. Buchlin, T. Sentenac and J.-J. Orteu.Shape Distortions Induced by Convective Effect on Hot Object in Visible, Near Infrared and Infrared Bands. *Experiments in Fluids*, vol. 54, p. 1452, 2013.
[20] P. Bertrand, C. Huchette, T. Archer, T. Vandellos and F. Hild. Mesure de longueur de fissure d'interface en température entre une barrière environnementale et un substrat composite à matrice céramique. In *Journées Nationales sur les Composites*, 2023.
[21] J. R. Rice. A Path Independent Integral and the Approximate Analysis of Strain Concentration by Notches and Cracks. *Journal of Applied Mechanics*, vol. 35, nº 2, p. 379-386, 1968.
[22] J. S. Lyons, J. Liu and M. A. Sutton. High-temperature deformation measurements using digital-image correlation. *Experimental Mechanics*, vol. 36, nº 1, p. 64-70, 1996.
[23] M. Berny, T. Archer, A. Mavel, P. Beauchêne, S. Roux and F. Hild. On the analysis of heat haze effects with spacetime DIC. *Optics and Lasers in Engineering*, vol. 111, p. 135-153, 2018.
[24] P. Leplay, O. Lafforgue and F. Hild. Analysis of Asymmetrical Creep of a Ceramic at 1350°C by Digital Image Correlation. *J. Am. Ceram. Soc.*, vol. 98, nº 7, p. 2240-2247, 2015.